Journal of Alloys and Compounds 504S (2010) S299–S301

Contents lists available at ScienceDirect

Journal of Alloys and Compounds

journal homepage: www.elsevier.com/locate/jallcom

Microstructural characterization and hydrogenation study of extruded MgFe alloy

G.F. Lima[a], M.M. Peres[a], S. Garroni[b], M.D. Baró[b], S. Surinyach[b], C.S. Kiminami[c], T.T. Ishikawa[c], W.J. Botta[c], A.M. Jorge Jr.[c,*]

[a] Post-Graduate Program in Materials Science and Engineering, Department of Materials Engineering, Federal University of São Carlos, São Carlos, SP, Brazil
[b] Universitat Autònoma de Barcelona, Barcelona, Spain
[c] Department of Materials Engineering, Federal University of São Carlos, Via Washington Luiz, km 235, 13565-905 São Carlos, SP, Brazil

ARTICLE INFO

Article history:
Received 28 June 2009
Received in revised form 3 March 2010
Accepted 9 March 2010
Available online 15 March 2010

Keywords:
Hydrogenation process
Hot extrusion
Mg alloy
Complex hydrides

ABSTRACT

Mg-based nanocrystalline alloys or nanocomposites are promising materials for hydrogen storage in the solid state, which is a more effective and safer storage medium than pressurized or liquefied hydrogen. Among the many Mg-based hydrides of interest for hydrogen storage, Mg_2FeH_6 is in a special position due to its relatively high gravimetric capacity of 5.5% and excellent volumetric density of 150 kg H_2/m^3. This work involved a study of the synthesis and processing of Mg-based alloys of this type, produced by high-energy ball milling and hot extrusion. A mixture of 2Mg–Fe was prepared by high-energy ball milling under argon gas. The resulting powder was cold-pressed to produce cylindrical pre-forms, which were then extruded and the sorption properties were analyzed in a microbalance and in a Sieverts apparatus. Phase formation, microstructural evolution, desorption temperatures, and hydrogen storage capacity were analyzed by X-ray diffraction, scanning electron microscopy (SEM), differential scanning calorimetry, and thermogravimetric techniques. The results showed that Mg_2FeH_6 was formed and the hydrogen reaction was reversible. SEM observations indicate a microstructure composed of nanosized grains in the range of 30–80 nm inside particles of about 50 μm, and Mg_2FeH_6 formed mainly at the particle interfaces. The desorption temperature started at about 225 °C, reaching a maximum at 440 °C with low capacity of absorption, indicating low absorption/desorption kinetics, probably due to bulk diffusion limitations.

1. Introduction

Mg-based alloys are a relatively light, low-cost and promising material for hydrogen storage due mainly to the high gravimetric and volumetric hydrogen capacities of their hydrides [1]. Among these alloys, MgH_2 has the highest gravimetric storage capacity (7.6 wt.% of H), while Mg_2FeH_6 presents the highest volumetric storage density (150 g of H_2/l, which is 9.1×10^{22} atoms of H/cm^3), i.e., twice the liquid state storage density, and its hydrogenation reaction is reversible and has high cyclic stability [2]. However, these alloys present high desorption temperatures and slow kinetics [3]. Nonconventional materials with nanocrystalline structures produced by high-energy ball milling (HEBM) exhibit higher storage capacities and faster hydrogen absorption and desorption kinetics than crystalline materials; moreover, nanocomposites may present even better hydrogen properties than each of their isolated components [3–7].

Currently, nonconventional processing routes involving severe plastic deformation (SPD) have proved to be promising techniques for the preparation of Mg alloys for bulk hydrogen storage. The improvements are: higher capacity, chemical stability, and kinetics; and an easier activation process or even its elimination [8–12]. However, these techniques produce small and very fragile samples, diminishing their usefulness in technological applications. In this paper we present the results of production of bulk Mg_2FeH_6, using the high-energy ball milling (HEBM) and hot extrusion process.

2. Experimental procedure

A mixture of 2Mg–Fe was prepared by high-energy ball milling, with ball to powder ratio of 20:1, under argon gas atmosphere. The resulting powder was cold-pressed to produce cylindrical pre-forms, which were then extruded (EXT) at 300 °C, with an extrusion ratio of 3/1 and ram speed of 1 mm/min. The extruded sample was cut into pieces and the sorption capacity was analyzed in an Air Product-VTI Rubotherm microbalance with an integrated mass spectrometer (five cycles at 400 °C, under 11 bar of H_2 for 5 h), and in a Sieverts apparatus (one cycle at 400 °C, under 30 bar of H_2 for 24 h).

The microstructural characterization was performed by scanning electron microscopy (Philips XL30 FEG-SEM). The phase characterization was performed by X-ray diffraction (XRD) using monochromatic Cu-Kα radiation with an angular pass of 0.032°, in a Siemens D5005 diffractometer equipped with a C-monochromator.

* Corresponding author. Tel.: +55 16 33518531; fax: +55 16 33615404.
E-mail address: moreira@ufscar.br (A.M. Jorge Jr.).

0925-8388/$ – see front matter © 2010 Elsevier B.V. All rights reserved.
doi:10.1016/j.jallcom.2010.03.101

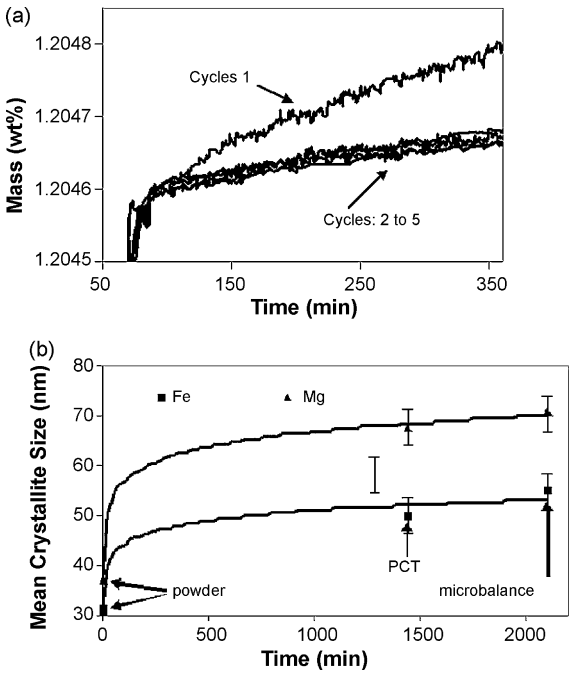

Fig. 1. (a) Hydrogenation and dehydrogenation microbalance results (five cycles at 400 °C, under 11 bar of H_2 for 5 h) and (b) crystallite size as a function of time of PCT and microbalance, both at 400 °C.

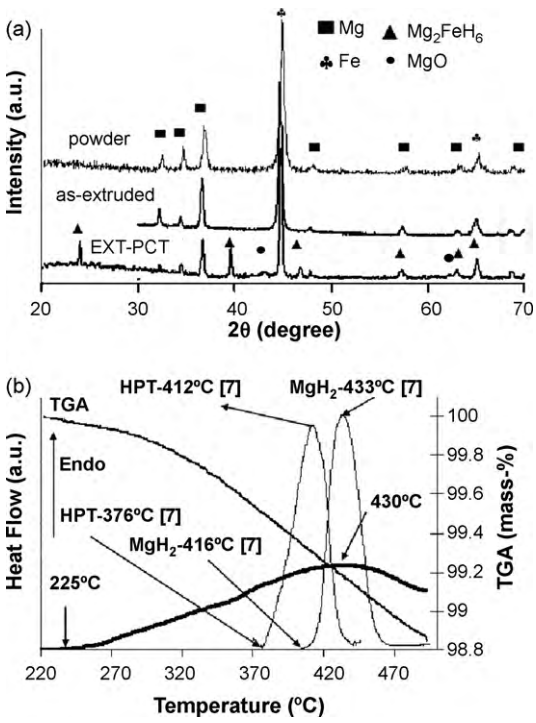

Fig. 3. (a) XRD patterns of the powder, the as-extruded (EXT) and the extruded PCT-hydrogenated (EXT-PCT). (b) DSC curves of: comparing the hydrogenated EXT-PCT, SPD-HPT-2Mg–Fe disk [7] and the commercial MgH_2 [7] alloys and TGA from EXT-PCT sample.

Rietveld refinement was used to analyze the XRD spectra to determine the crystallite size, phase identification and phase proportion, using Maud software (www.ing.unitn.it/~maud/index.html). The extruded sample was hydrogenated (EXT-PCT) in a Sieverts apparatus and was heated in a Perkin Elmer DSC/TG-7 differential scanning calorimeter/thermogravimetric analyzer. Hydrogen desorption temperatures were measured during continuous heating of the hydrides at heating rates of 2, 3.5, 5 and 10 °C/min, using purified and dried argon gas in an overflow regime. The apparent activation energy was calculated from the DSC data using an adapted Kissinger equation [13].

3. Results and discussion

After extrusion the samples presented high mechanical strength, suggesting that this type of processing can be considered superior to other consolidation processes which result in brittle samples. Hydrogen storage materials with higher mechanical strength are expected to show better shape stability to thermal cycling.

Fig. 1a shows the results from microbalance after five cycles of hydrogenation and dehydrogenation, and Fig. 1b the mean crystallite size (obtained from XRD after Rietveld refinement) as a function of time. From these graphs, it is interesting to note that the initial crystallite size is only relevant in the first cycle, i.e., when the crystallite size was about 38 nm (Fe) and 52 nm (Mg) (as-extruded samples) the volumetric hydrogen capacity increased. Also, during crystallite growth (next four cycles) the volumetric capacity remains unchanged. It is worth noting that the increase in volumetric capacity is only 0.06%. Also, it is very important to note the pinning effect of iron, as shown in Fig. 2d, which reduces Mg grain growth and contributes to complex hydride formation (Fig. 3a).

Fig. 2 shows a sequence of FEG-SEM images (BSE mode) of an EXT-PCT transversal section. Fig. 2a–c indicates that the (darker areas) preferential sites of hydrogenation are the pores and adjacent areas at particle interfaces. Fig. 2b shows the presence of particles with a mean size of 50 μm. The high porosity and adjacent areas covers about 20% of the transversal section area. Additionally, Fig. 2d shows that there are still unreacted Fe particles (white particles) inside the hydrogenated region, pinning the other particles. The mean size of these particles is similar to that of the bcc-Fe observed in Fig. 1b, which are on average about 70 nm.

Fig. 3a shows the XRD patterns of the as-extruded and EXT-PCT samples compared with that of the precursor powder. The peaks were identified as hcp-Mg and bcc-Fe solid solutions in all the samples and as Mg_2FeH_6 phase in the EXT-PCT sample. After Rietveld refinement, the phase proportion in the EXT-PCT sample was calculated as 58.6% Mg, 12.7% Fe, 5.6% MgO and 23.1% Mg_2FeH_6, indicating that about 1% of hydrogen was absorbed by the specimen, i.e., about 20% of the maximum capacity of the Mg_2FeH_6 complex hydride.

Fig. 3b compares the DSC analyses of EXT-PCT, SPD-HPT-2Mg–Fe [7] and commercial MgH_2 [7]. The endothermic peak corresponding to H_2 desorption in the EXT-PCT started at about 225 °C, as

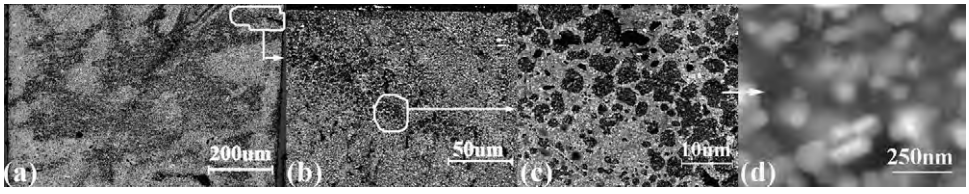

Fig. 2. Sequence of FEG-SEM images (BSE mode) of an EXT-PCT transversal section. (a–c) Darker areas indicating the preferential sites of hydrogenation and (d) pinning effect of the iron particles (brighter) inside the hydrogenated region, pinning the other particles.

compared with 376 °C for the SPD-HPT-2Mg–Fe, and 416 °C for the MgH_2 samples. The apparent activation energy for the desorption process can be calculated from this figure. The apparent activation energies for dehydrogenation of pure and Fe-doped magnesium hydrides were $E_A \approx 354$ kJ/mol for MgH_2, 334 for SPD-HPT-2Mg–Fe, and 350 for EXT-PCT. The relatively high activation energies are probably due to magnesium oxide surface layers, which retard the diffusion of hydrogen from MgH_2/Mg and Mg_2FeH_6/Mg. Notwithstanding the catalytic effect of Fe on the recombination of H atoms to hydrogen molecules – which produced the difference of 20 kJ/mol in the SPD-HPT-2Mg–Fe sample – here this effect was strongly hampered by the larger volume of the EXT-PCT compared to that of the SPD-HPT-2Mg–Fe sample. These energy results show that the addition of Fe may be expected to lower the dissociation barrier for H_2 significantly, thus reducing the starting temperature for dehydrogenation. The reduction on the starting temperature was more pronounced in the EXT-PCT sample, probably due to differences in porosity (Fig. 2).

The reaction of metals, as for example Mg, with hydrogen consists of several steps: (i) nucleation and growth of Mg, (ii) diffusion of hydrogen in bulk Mg/MgH_2–Mg/Mg_2FeH_6, (iii) surface penetration, e.g., through MgO, for oxidized samples, (iv) two-dimensional surface diffusion of H, and (v) recombination of 2H to H_2, a catalyzed process. Furthermore, (vi) cation migration in alloys induced by hydrogenation or dehydrogenation may also be important during phase formation/separation. The rate-determining step accounts for the largest contribution to the apparent activation energy. This may indicate that the dissociation of H_2 and the recombination of H to H_2 occur mainly in association with iron due to its lower barrier compared to that of pure magnesium, even in the presence of a very small percentage of Fe. Like magnesium, iron is oxidized in air to form FeO oxide. Unlike MgO, FeO is readily reduced by hydrogen gas. This appears to suggest that the main role of Fe may be to catalyze the dissociation/recombination reaction barrier for H_2 while exerting a minor influence on the other processes, as clearly indicated by the differences in the kinetics of the three samples shown in Fig. 3b. The data seem to indicate a nucleation period prior to the onset of dehydrogenation. As this figure indicates, the incubation time of the MgH_2 sample is longer than that of the Fe-doped samples. However, the faster dehydrogenation kinetics of the MgH_2 and the SPD-HPT-2Mg–Fe samples is visible in the DSC curves, which again can be explained by the larger volume of the EXT-PCT sample compared to that of the SPD-HPT-2Mg–Fe or MgH_2 samples. Also, note that desorbed hydrogen (TGA) was about 1.2%, which is in agreement with the results (1%) calculated from the XRD patterns shown in Fig. 3a.

4. Conclusions

Complex hydrides were produced successfully in bulk samples by a high-energy ball milling and hot extrusion process. Besides the physical determining aspects related to H_2 desorption, sample porosity and the interface between particles have high contribution in the hydrogen desorption properties.

The iron in the 2Mg–Fe mixture produced a beneficial pinning effect on the Mg grains, resulting in modest grain growth, even when the sample was maintained in high temperatures for long periods.

Hydrogen absorption and desorption kinetics were improved by the addition of iron in magnesium, producing a catalytic effect that lowered the desorption temperature. The incubation time to start the H_2 desorption process was longer in the MgH_2 sample than in the Fe-doped one.

The desorption kinetics of samples processed by high pressure torsion (HPT) was faster than that of extruded samples, probably due to bulk diffusion limitations.

The activation energy values for the desorption processes were relatively high, possibly due to oxide layers on the samples' surfaces. The lower activation energy of the Fe-doped samples suggests that the recombination of H to H_2 was catalyzed by Fe.

Acknowledgements

The authors are acknowledged for financial support from FAPESP, CAPES and CNPq. S.G. is acknowledged for support from the European Commission under MRTN-Contract "Complex Solid State Reactions for Energy Efficient Hydrogen Storage" (MRTN-CT-2006-035366).

References

[1] A. Züttel, P. Wenger, P. Sudan, P. Mauron, S.-I.S.-I. Orimo, Mater. Sci. Eng. B 108 (2004) 9–18.
[2] B. Bogdanović, A. Reiser, K. Schlichte, B. Spliethoff, B. Tesche, J. Alloys Compd. 345 (2002) 77–89.
[3] J.J. Didisheim, P. Zolliker, K. Yvon, P. Fischer, J. Schefer, M. Gubelmann, A.F. Williams, Inorg. Chem. 23 (1984) 1953–1957.
[4] B. Sakintuna, F. Lamari-Darkrimb, M. Hirscher, Int. J. Hydrogen Energy 32 (2007) 1121–1140.
[5] M. Porcu, A.K. Petford-Long, J.M. Sykes, J. Alloys Compd. 453 (2008) 341–346.
[6] N. Hanada, E. Hirotoshi, T. Ichikawa, E. Akiba, H. Fujii, J. Alloys Compd. 450 (2008) 395–399.
[7] G.F. Lima, A.M. Jorge Jr., D.R. Leiva, C.S. Kiminami, C. Bolfarini, W.J. Botta, J. Phys.: Conf. Ser. 144 (2009) 012015.
[8] T.T. Ueda, M. Tsukahara, Y. Kamiya, S. Kikuchi, J. Alloys Compd. 386 (2005) 253–257.
[9] J. Dufour, J. Huot, J. Alloys Compd. 439 (2007) L5–L7.
[10] J. Dufour, J. Huot, J. Alloys Compd. 446–447 (2007) 147–151.
[11] N. Takeichi, K. Tanaka, H. Tanaka, T.T. Ueda, Y. Kamiya, M. Tsukahara, H. Miyamura, S. Kikuchi, J. Alloys Compd. 446–447 (2007) 543–548.
[12] Y. Kusadome, K. Ikeda, Y. Nakamori, S. Orimo, Z. Horita, Scr. Mater. 57 (2007) 751–753.
[13] H.E. Kissinger, Anal. Chem. 29 (1957) 1702–1706.